Colon Crypts of Subjects With Familial Adenomatous Polyposis Show an Increased Number of LGR5+ Ectopic Stem Cells

Lucas T. Jennelle, PhD[1], Christopher H. Dampier, MD[1,2], Stephanie Tring, BS[3], Steven Powell, MD[4] and Graham Casey, PhD[1]

INTRODUCTION: **Familial adenomatous polyposis (FAP) is a hereditary colorectal cancer (CRC) syndrome characterized by accelerated adenoma development due to inherited (or *de novo*) mutations in the APC regulator of WNT signaling pathway (*APC*) gene. The mechanism underlying this accelerated polyp development in subjects with FAP has not been defined. Given that LGR5+ stem cells drive crypt cell proliferation, we hypothesized that FAP crypts would demonstrate aberrant leucine-rich repeat–containing G-protein–coupled receptor 5 (LGR5) staining patterns.**

METHODS: **Biopsies were taken from 11 healthy subjects, 7 subjects with Lynch syndrome, 4 subjects with FAP, and 1 subject with *MUTYH*-associated polyposis syndrome during routine screening or surveillance colonoscopy. Crypt staining was evaluated by immunohistochemistry of paraffin-embedded tissue sections. Stem cell numbers were estimated by immunofluorescence staining of isolated crypts using antibodies against LGR5 and other proteins.**

RESULTS: **Subjects with FAP exhibited a greater number of LGR5+ stem cells in their crypts than healthy subjects and subjects with Lynch syndrome and *MUTYH*-associated polyposis syndrome. Most crypts of subjects with FAP harbored LGR5+ cells located above the lower third of the crypts.**

DISCUSSION: **These findings support a model in which inactivation of one copy of *APC* leads to increased numbers of LGR5+ stem cells, many of which are ectopic, in colon crypts of subjects with FAP. Overabundant and ectopic LGR5+ stem cells could lead to an expanded proliferative zone of dividing cells more likely to develop mutations that would contribute to the accelerated adenoma development observed in FAP.**

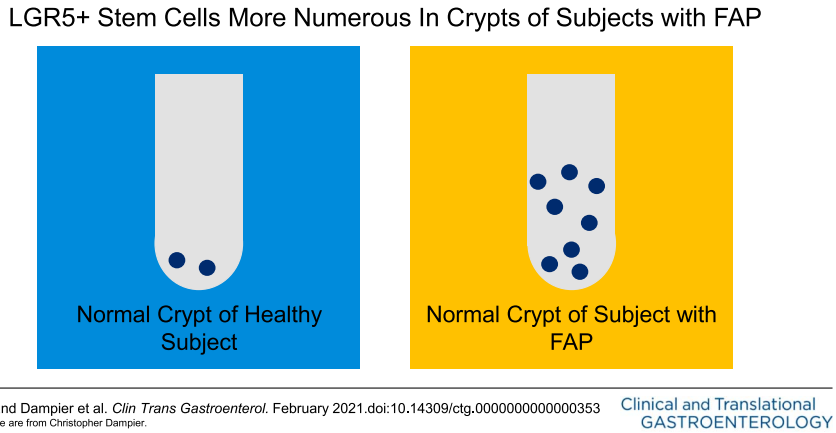

Jennelle and Dampier et al. *Clin Trans Gastroenterol.* February 2021.doi:10.14309/ctg.0000000000000353
All icons above are from Christopher Dampier.
Clinical and Translational GASTROENTEROLOGY

[1]Center for Public Health Genomics, Department of Public Health Sciences, University of Virginia, Charlottesville, Virginia, USA; [2]Department of General Surgery, University of Virginia, Charlottesville, Virginia, USA; [3]USC Genomics Core, University of Southern California, Los Angeles, California, USA; [4]Division of Gastroenterology & Hepatology, Department of Medicine, University of Virginia, Charlottesville, Virginia, USA. **Correspondence:** Graham Casey, PhD. E-mail: gc8r@virginia.edu.

Received August 7, 2020; accepted March 29, 2021; published online May 17, 2021

SUPPLEMENTARY MATERIAL accompanies this paper at http://links.lww.com/CTG/A612; http://links.lww.com/CTG/A613; http://links.lww.com/CTG/A614; http://links.lww.com/CTG/A615; http://links.lww.com/CTG/A616; http://links.lww.com/CTG/A617

Clinical and Translational Gastroenterology 2021;12:e00353. https://doi.org/10.14309/ctg.0000000000000353

INTRODUCTION

Tissue stem cells replenish differentiated cells during homeostatic turnover and rebuild tissue after injury, maintaining a tissue's long-term renewal capacity (1,2). However, the sentinel property of tissue stem cells, self-renewal, can become dysregulated, bypass intrinsic checkpoints, and lead to transformation and autonomous growth (3). The colon has immense regenerative capacity, replacing its billions of epithelial cells approximately every 5 days (1,2). Examination of stem cells in hereditary colorectal cancer (CRC) syndromes such as familial adenomatous polyposis (FAP) can highlight important cellular changes preceding onset of CRC (3,4).

Colon crypts contain a dedicated stem cell compartment, and several molecular markers of colon stem cells have been proposed, including ASCL2, ALDH1, BMI1, CD24, CD44, CD133, CD166, LRIG1, MSI1, OLFM4, and PTK7. These markers have confirmed the base of the colon crypt as the stem cell niche (2,5–15). Recent evidence indicates that leucine-rich repeat–containing G-protein–coupled receptor 5 (LGR5), a transmembrane receptor that potentiates the canonical WNT signaling pathway, is the most specific and reliable marker of pluripotent cells in the colon. Protein immunostaining and transcript hybridization studies demonstrate that LGR5 is found exclusively in a minority of cells at the crypt base in healthy colon (16–20). Lineage tracing studies in mice demonstrate that LGR5+ cells give rise to all cell lineages observed in the colon crypt (16,21). Furthermore, isolated LGR5+ cells from mice and humans can lead to the generation of self-sustaining colon organoids (22,23). For these reasons, LGR5 has emerged as the best marker of stem cells in the colon.

FAP is caused by inherited or *de novo* germline mutations in the gene encoding the adenomatous polyposis coli (APC) protein, which is involved in cell proliferation and differentiation. Mutation carriers develop multiple adenomatous polyps in the colon and rectum, typically beginning in the second decade of life (24). By the third decade of life, approximately 95% of trait carriers have polyps, often in the hundreds to thousands. Nearly all subjects with FAP develop microsatellite stable CRC by an average age of 45 years (3,25). Lynch syndrome and *MUTYH*-associated polyposis (MAP) are 2 other hereditary CRC syndromes. Lynch syndrome is caused by inherited germline mutations in one of several genes encoding DNA mismatch repair proteins. *MUTYH*-associated polyposis (MAP) is caused by inherited biallelic germline mutations in the mutY DNA glycosylase (*MUTYH*) gene, which encodes a base excision repair protein. Patients with Lynch syndrome or MAP do not manifest the accelerated adenomatous polyp development observed in FAP, although patients with MAP may present with multiple polyps.

Despite knowledge of the genetic basis of FAP, the mechanism underlying the accelerated polyp development is not well understood. Previous studies have suggested that nonneoplastic crypts from subjects with FAP harbor an expanded proliferative zone compared with healthy controls (16,26–28). Given that LGR5+ stem cells drive crypt cell proliferation, we hypothesized that crypts from subjects with FAP would demonstrate aberrant LGR5 staining patterns compared with crypts from healthy subjects. Based on clinical manifestations, we expected crypts from subjects with Lynch syndrome and MAP to demonstrate a similar staining pattern to that of healthy subjects.

METHODS

Subject enrollment

Subjects undergoing screening or surveillance colonoscopy at the Digestive Health Center of the University of Virginia Health System (UVA) during the period September 2017 to December 2019 were enrolled under an approved Institutional Review Board for Health Sciences Research protocol after obtaining informed consent (IRB-HSR#19439). Subjects were considered healthy when they were without symptoms and a personal history of CRC, inflammatory bowel disease, or other known colon pathology and when they had no more than 2 tubular adenomas, each fewer than 10 mm in diameter. Both men and women were considered for enrollment. Ultimately, 11 healthy subjects were included (age range 52–74 years) (Table 1). Subjects with a clinical diagnosis of FAP, Lynch syndrome, or MAP for whom confirmatory molecular genetic test results were available in the

Table 1. Clinical and epidemiologic information

Subject ID	Sex	Age (yr)	Diagnosis	Figure
H1	Female	52	Healthy	1a, 1b
H2	Female	74	Healthy	
H3	Male	70	Healthy	1c
H4	Male	56	Healthy	
H5	Female	65	Healthy	2
H6	Female	52	Healthy	
H7	Male	66	Healthy	4a
H8	Female	63	Healthy	4b
H9	Female	62	Healthy	S2a, S3a
H10	Male	72	Healthy	S4a
H11	Male	74	Healthy	S4b
L1	Female	63	Lynch syndrome	S4d
L2	Female	81	Lynch syndrome	
L3	Female	39	Lynch syndrome	
L4	Female	21	Lynch syndrome	2
L5	Female	66	Lynch syndrome	
L6	Female	31	Lynch syndrome	
L7	Female	37	Lynch syndrome	
M	Male	59	*MUTYH*-associated polyposis	S4d
F1	Female	48	Familial adenomatous polyposis	2
F2	Male	24	Familial adenomatous polyposis	
F3	Female	47	Familial adenomatous polyposis	4d
F4	Male	19	Familial adenomatous polyposis	4c, S2b, S3b

Table 2. Antibodies for immunostains

Antigen	Source	Species	Clone	Dilution	Type	Figure
CD44v6	eBioscience	Mouse mAb	VFF-18	1:200	IHC	S2
Chromogranin A	Agilent/DAKO	Rabbit pAb	A0430	1:500	IHC	S2
Cytokeratin 20	Agilent/DAKO	Mouse mAb	Ks20.8	1:20	IHC	S2
Ki67	Abcam	Rabbit mAb	SP6	1:400	IHC	S2
LGR5	Miltenyi	Rabbit mAb	STE-1-89-11.5	1:50	IHC	S3
OLFM4	Cell Signaling	Rabbit mAb	D1E4M	1:100	IHC	S2
BMI1	Miltenyi	Human IgG1	REA438	1:10	IF	4
β-Catenin	Miltenyi	Human IgG1	REA480	1:100	IF	
Act.-β-catenin	EMD Millipore	Mouse mAb	8E7	1:100	IF	
CD24	BioLegend	Mouse mAb	ML5	1:50	IF	S4
CD44	Tonbo	Rat mAb	IM7	1:800	IF	1, S4
CD66a	eBioscience	Mouse mAb	CD66a-B1.1	1:200	IF	1, S4
LGR5	Miltenyi	Human IgG1	REA762	1:500	IF	1, 2, 4, S4
LGR5	Origene	Mouse mAb	OTI2A2	1:100	IF	S4b
LRIG1	R&D	Mouse mAb	FAB7498	1:100	IF	4

IHC, immunohistochemistry; IF, immunofluorescence.

electronic medical record were considered for inclusion. Mutation carriers were considered for inclusion when they had intact proximal or distal colon for evaluation. Ultimately, 4 subjects with FAP (age range 19–48 years), 7 subjects with Lynch syndrome (age range 21–81 years), and 1 subject with MAP (age 59 years) were included (Table 1). All methods were performed in accordance with relevant guidelines and regulations and were consistent with those required by both the National Institutes of Health and UVA.

Sample collection

Biopsy collection from normal-appearing colon mucosa was conducted using jumbo (for paraffin embedding) or standard (for crypt isolation) endoscopic forceps. For healthy subjects, biopsies were collected within 5 cm of the hepatic flexure (right colon) or within 5 cm of the splenic flexure (left colon). For mutation carriers, biopsies were collected from uninvolved, normal-appearing mucosa, regionally similar to that used for healthy subjects.

Biopsies for immunohistochemistry were placed into nylon bags, secured in a cassette, and immersed in 10% neutral-buffered formalin (VIP Fixative; SciGen, Paramount, CA) for 24 hours. After fixation, samples were dehydrated in 70% ethanol overnight before paraffin embedding at the Biorepository and Tissue Research Facility at UVA. Biopsies for immunofluorescence were placed directly into cold collection media (Advanced DMEM/F-12, 10% FBS, HEPES, penicillin–streptomycin, L-glutamine, and GlutaMax) on ice before crypt isolation.

Crypt isolation

Biopsies for immunofluorescence were washed with cold phosphate-buffered saline (PBS) within 30 minutes of collection and incubated for 20 minutes in 9 mM EDTA in PBS with gentle mixing. During the incubation, crypts separated from villous material and settled by gravity. Crypts were then collected by low-speed centrifugation (1,200 rpm for 5 minutes) and mixed with Matrigel (Corning). Finally, crypts were plated in individual wells of an 8-well chamber slide (Lab-Tek II, Nunc), and after solidification of Matrigel, domes were briefly hydrated with collection media before fixation.

Immunohistochemical staining

Immunohistochemical staining of formalin-fixed paraffin-embedded tissue was performed in the Biorepository and Tissue Research Facility on a robotic platform (Ventana Discover Ultra Staining Module; Ventana, Tucson, AZ). Tissue sections (4 μm) were deparaffinized using EZ Prep solution (Ventana). A heat-induced antigen retrieval protocol (64 minutes) was performed using Cell Conditioner 1 (Ventana). Endogenous peroxidases were blocked with peroxidase inhibitor (CM1, 8 minutes) before incubation with antibodies for CD44v6 (eBioscience), chromogranin A (Agilent/DAKO), cytokeratin 20 (Agilent/DAKO), Ki67 (Abcam), LGR5 (Miltenyi), or OLFM4 (Cell Signaling) (Table 2) for 60 minutes at room temperature. Justification for specific antibodies used is provided in the Supplementary Methods (see Supplementary Digital Content 1, http://links.lww.com/CTG/A612). Antigen–antibody complex was detected using DISCOVERY OmniMap anti-mouse multimer for CD44v6 and cytokeratin 20 and DISCOVERY ChromoMap DAB kit (Ventana) with anti-rabbit conjugate for chromogranin A, Ki67, LGR5, and OLFM4. All slides were counterstained with hematoxylin, dehydrated, cleared, and mounted for assessment.

Immunofluorescence staining

Immunofluorescence staining was conducted as described by Mahe et al. (23). After collection medium was removed, crypts were fixed with 4% paraformaldehyde and permeabilized with Triton X-100 (0.1% in PBS). They were washed with PBS before fixation and again before permeabilization. After permeabilization, crypts were

Table 3. LGR5+ cell counts

Subject ID	Sex	Age (yr)	Diagnosis	Crypts scored	LGR5+ mean	LGR5+ SD
H1	Female	52	Healthy	7	2.4	1.0
H2	Female	74	Healthy	9	2.2	0.7
H3	Male	70	Healthy	4	2.8	1.0
H4	Male	56	Healthy	2	1.5	0.7
H5	Female	65	Healthy	10	2.2	0.9
H6	Female	52	Healthy	9	2.1	0.8
H7	Male	66	Healthy	4	1.5	0.6
H8	Female	63	Healthy	10	1.5	0.9
H9	Female	62	Healthy	4	2.0	0.8
H10	Male	72	Healthy	10	1.7	0.7
L1	Female	63	Lynch	2	2.5	0.7
L2	Female	81	Lynch	5	2.8	0.4
L3	Female	39	Lynch	3	2.0	1.0
L5	Female	66	Lynch	7	1.4	0.6
L6	Female	31	Lynch	2	2.5	2.1
L7	Female	37	Lynch	14	2.4	0.9
F1	Female	48	FAP	2	6.8	2.5
F2	Male	24	FAP	5	5.0	1.0
F3	Female	47	FAP	4	4.0	2.2
F4	Male	19	FAP	7	2.4	0.6

FAP, familial adenomatous polyposis; LGR5, leucine-rich repeat–containing G-protein–coupled receptor 5.

blocked with blocking buffer (1% BSA, 3% normal goat serum, and 0.2% Triton X-100 in PBS) and incubated with antibodies for BMI1 (Miltenyi), β-catenin (Miltenyi), activated β-catenin (EMD Millipore), CD24 (BioLegend), CD44 (Tonbo), CD66a (eBioscience), LGR5 (Miltenyi and Origene), or LRIG1 (R&D) (Table 2) in working buffer (0.1% BSA, 0.3% normal goat serum, and 0.2% Triton X-100 in PBS) before mounting (Fluoromount-G, SouthernBiotech) for observation. Crypts were washed with PBS before blocking, incubation, and mounting. Justification for specific antibodies used is provided in the Supplementary Methods (see Supplementary Digital Content 1, http://links.lww.com/CTG/A612). Note that 2 separate LGR5 antibodies were tested for immunofluorescence.

Confocal microscopy and image capture

Microscopy was performed using a Zeiss LSM880 Laser Scanning Confocal Microscope. To maintain consistency across microscopy experiments on different days, laser intensities for each microscope channel were stored in a baseline confocal file used to restore original brightness and contrast settings for each session. Despite consistent laser settings, variability in background signal was not completely eliminated because of variability in crypt depth within Matrigel domes and concomitant variability in reflection and refraction of ambient Matrigel.

For each subject, preliminary examination of immunofluorescence staining was performed by a single operator (L.T.J.). Every Matrigel dome was evaluated in multiple focal planes, and approximately 10 intact crypts were inspected before selection for imaging. Crypts reflective of the population found in each dome were imaged. Images of single focal planes were collected for every subject. A subset of FAP, healthy, and Lynch syndrome crypts were imaged in multiple focal planes across varying depths and rendered in Z-stacks.

After acquisition, digital images of all crypts were processed by a single operator (L.T.J.) using ImageJ software. Brightness and contrast were not manipulated except in 2 cases: (i) Z-stack rendering, for which the maximum intensity Z-projection method was used, and (ii) preparation for crypt scoring (i.e., counting of LGR5+ cells). For the purpose of scoring, brightness and contrast were selected for crypts individually to maintain as much crypt architecture as possible while prioritizing isolation of true LGR5+ signals.

Quantification of LGR5+ cells

Only images of single focal planes were used to quantify LGR5+ cells. All processed images of intact, full-length crypts were deidentified (i.e., subject and diagnostic labels were removed) and randomized by a single observer (C.H.D.). Images (n = 122) were scored independently by 2 observers (C.H.D. and an impartial observer with no other participation in this study), both blinded to the clinical diagnosis of subjects from whom crypts had been isolated at the time of scoring. Two images were excluded during scoring because of observer disagreement about crypt borders. The microscope operator (L.T.J.) who captured the images was excluded from scoring.

Images were scored for total LGR5+ cells and ectopic LGR5+ cells. Ectopic LGR5+ cells were defined by dividing the length of each crypt into approximate thirds by visual inspection and labeling any LGR5+ cells located in the upper two-thirds of the crypt as ectopic. Interobserver variability for total and ectopic counts was assessed with linear regression and Bland-Altman plots (see Supplementary Figure 1, Supplementary Digital Content 2, http://links.lww.com/CTG/A613). To establish consensus counts for the final quantifications used in statistical analysis, the mean of the 2 blinded counts was calculated for each crypt. One healthy subject (H11) and 1 subject with Lynch syndrome (L4) were excluded from scoring because of insufficient images of intact, full-length crypts. The single subject with MAP was excluded from scoring because of insufficient subjects in the same diagnostic category to support generalizable quantitative inferences.

Statistical analysis

For association tests of total LGR5+ cell counts, count was modeled as the response variable in generalized estimating equations in which colon location, subject age, subject clinical diagnosis, or subject age and clinical diagnosis together were used as explanatory variables. Subject identifier was used to identify clusters, and the working correlation structure was specified as exchangeable. For tests of colon location and subject age, 69 crypts from 10 healthy subjects (41 from proximal and 28 from distal colon) were used. For tests involving clinical diagnosis, 120 crypts from 20 subjects (69 from 10 healthy subjects, 33 from 6 subjects with Lynch syndrome, and 18 from 4 subjects with FAP) were used. All tests were performed in R using geepack (29–32). Generalized estimating equations are appropriate in this setting because they efficiently account for clustered data (33). In this

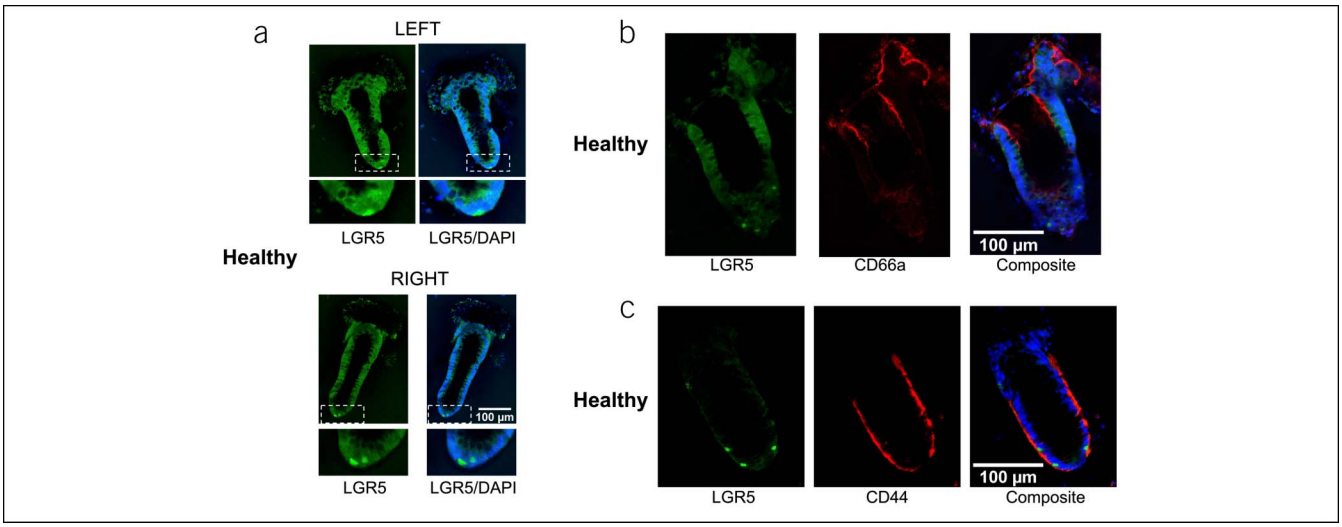

Figure 1. LGR5 staining in crypts of healthy subjects. LGR5 expression and localization in normal colon crypts of healthy subjects. Blue is nuclear DNA counterstained with DAPI. (**a**) Immunofluorescence of LGR5 in crypts from left and right colon (same scale). (**b**) Immunofluorescence of differentiated cell marker CD66a and LGR5. (**c**) Immunofluorescence of proliferating cell marker CD44 and LGR5. Objective: 20×. Scale bar: 100 µM. DAPI, 4′,6-diamidino-2-phenylindole; LGR5, leucine-rich repeat–containing G-protein–coupled receptor 5.

study, the LGR5+ cell count for a given subject is estimated from repeated measurements across multiple crypts. Individual crypts are clustered by subject, and the correlation among values for a given subject must be taken into account. For visualization of LGR5+ cell numbers per subject and per crypt, dot plots overlaid with group mean and standard deviation and histograms overlaid with jittered crypt level cell counts were generated in R using ggplot2 (34). Source code and raw data for statistical tests and plots are available on GitHub through the following URL: https://github.com/dampierch/lgr5-IF.

RESULTS

Limited number of LGR5+ cells at the base of crypts from healthy subjects

Normal tissue architecture and differentiation was seen after immunohistochemical staining of paraffin-embedded tissues of healthy subjects and subjects with FAP (see Supplementary Figures 2 and 3, Supplementary Digital Contents 3, http://links.lww.com/CTG/A614 and 4, http://links.lww.com/CTG/A615). Although weak LGR5 staining was observed at the base of crypts from both groups, it was not sufficiently discrete to permit accurate quantification of stem cells in either group. To overcome the limitations of our immunohistochemistry stains, we interrogated the number of LGR5+ cells in colon crypts using immunofluorescence. In all healthy subjects, staining consistently revealed between 1 and 3 LGR5+ cells, usually confined to the crypt base (Table 3; Figures 1 and 2a). Three of 69 (4%) healthy crypts had 4 LGR5+ cells, and 26 (38%) had LGR5+ cells located above the lower third of the crypt. None had more than 4 LGR5+ cells. No statistically significant associations were observed between LGR5+ cell counts and either colon location or subject age ($P = 0.4$ and $P = 0.8$, respectively).

To confirm our LGR5+ stain was marking crypt base stem cells, multicolor immunofluorescence staining with antibodies for LGR5, CD24, CD44, and CD66a was performed. Staining for CD66a, which marks differentiated cells, was mostly concentrated at the top of crypts, and staining for CD24 and CD44, which mark cells in the proliferative zone, was concentrated at the crypt base (Figure 1b,c; see Supplementary Figure 4a–c, Supplementary Digital Content 5, http://links.lww.com/CTG/A616). Staining for LGR5 was usually limited to cells in the crypt base. Staining for CD66a and CD24 was most prominent on the apical surface of cells, staining for CD44 was most prominent on the basolateral surface, and staining for LGR5 was most prominent in the cytoplasm. These results are consistent with previous reports (5,6,8,35).

To further verify the accuracy of our LGR5 stain, multicolor immunofluorescence with the same antibody for CD44 but a different antibody for LGR5 was performed. Staining again demonstrated CD44 concentrated at the crypt base on the basolateral surface of cells and LGR5 in the cytoplasm of a few cells at the crypt base (see Supplementary Figure 4b, Supplementary Digital Content 5, http://links.lww.com/CTG/A616).

Quantitative increase and ectopic location of LGR5+ cells in crypts of subjects with FAP but not Lynch syndrome

The number of LGR5+ cells in crypts of subjects with FAP and 2 other hereditary CRC syndromes, Lynch syndrome and MAP, was evaluated by immunofluorescence staining. Crypts from subjects with FAP demonstrated a greater number of total LGR5+ cells than crypts of healthy subjects ($P = 4.9e-04$) and subjects with Lynch syndrome ($P = 1.9e-03$), and many LGR5+ cells were located above the crypt base (i.e., lower third) (Tables 3 and 4; Figures 2 and 3; see Supplementary Figure 5a, Supplementary Digital Content 6, http://links.lww.com/CTG/A617). FAP crypts harbored higher numbers of LGR5+ cells than crypts of a single subject with MAP, but this observation needs to be verified in additional subjects with MAP (see Supplementary Figure 4d, Supplementary Digital Content 5, http://links.lww.com/CTG/A616). Nine of 18 (50%) FAP crypts had 4 or more LGR5+ cells, and 12 (66%) had LGR5+ cells located above the lower third of the crypt. A small increase in the average number of

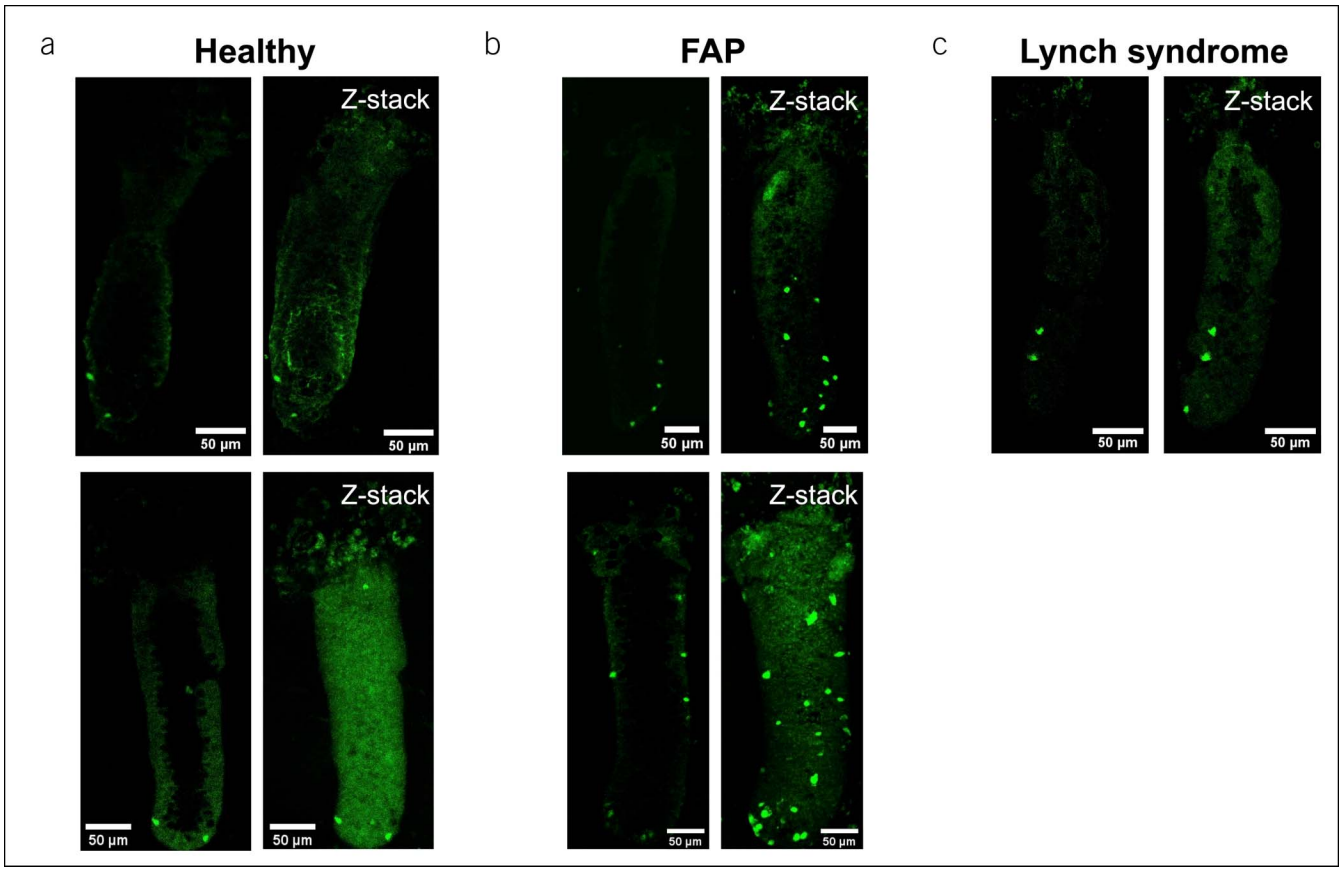

Figure 2. LGR5 staining in crypts of a healthy subject and subjects with CRC predisposition syndromes. LGR5 expression and localization in colon crypts. Immunofluorescence of LGR5 in crypts of 1 healthy subject, 1 subject with FAP, and 1 subject with Lynch syndrome. For each disease category, representative images of a single focal plane (left) and a Z-stack (right) of the same crypt are shown. (**a**) LGR5 staining in healthy crypts. The Z-stack of the crypt in the second row demonstrates a rare ectopic LGR5+ cell. (**b**) LGR5 staining in crypts of a subject with FAP. The Z-stack of the crypt in the second row demonstrates approximately 20 LGR5+ cells. (**c**) LGR5 staining in a crypt of a subject with Lynch syndrome. Objective: 20×. Scale bar: 50 μM. FAP, familial adenomatous polyposis; LGR5, leucine-rich repeat–containing G-protein–coupled receptor 5.

LGR5+ cells in crypts of subjects with Lynch syndrome relative to healthy subjects was not statistically significant ($P = 0.26$) (Table 4).

To assess the possibility that the observed increase in LGR5+ cell numbers in FAP crypts was because of younger age in subjects with FAP relative to healthy subjects, age was included as a covariate in the model used to test for count differences between groups. The effect of age was insignificant ($P = 0.3$) (Table 4). Furthermore, a linear model that predicts LGR5+ cell number based on subject age was fit using healthy subjects, and 3 of the 4 subjects with FAP demonstrated large, positive deviations from the LGR5+ cell counts predicted from their ages (see Supplementary Figure 5b, Supplementary Digital Content 6, http://links.lww.com/CTG/A617).

Of the 4 FAP subjects under investigation, 1 (F4) did not manifest the same level of overabundance of total or ectopic LGR5+ cells observed in the other 3. This was a surprising finding because the subject of interest was a first-degree relative of one of the other 3 and had inherited the same germline mutation in *APC*. The fact that this subject was 5 years younger than any other member of the FAP cohort and nearly 2 decades younger than the subject's first-degree relative with the same mutation but with a more extreme immunofluorescence phenotype raises the possibility that the increased LGR5+ staining phenotype is age dependent. Further studies will be required to test this hypothesis.

Qualitative assessment of LGR5+ cells in crypts of subjects with FAP

A striking observation in the FAP cohort was the necessity to examine multiple focal planes of a single crypt to identify all LGR5+ cells in that crypt. This finding was not formally quantified but was demonstrated in composite Z-stack images (i.e., stacks of images of single focal planes rendered as composite representations of entire crypts) obtained for a subset of subjects (Figure 2). The Z-stack images revealed markedly higher numbers of LGR5+ cells in crypts of subjects with FAP compared with images of single focal planes. Similar Z-stack images from healthy subjects and subjects with Lynch syndrome did not reveal noticeably higher numbers of LGR5+ cells relative to images of single focal planes. Based on this qualitative observation, we believe that the true number of LGR5+ cells in the crypts of subjects with FAP is higher than what we were able to report in Table 3.

To determine whether LGR5+ cells in crypts of subjects with FAP had other qualitative differences from those in crypts of healthy subjects, 2-color immunofluorescence staining was performed with antibodies for LGR5 and either BMI1 or LRIG1 in 2

Table 4. Parameter estimation for GEE model fit

	LGR5+ cell count			
Predictor	**Estimate**	**SE**	**Wald**	***P***
Intercept	1.14	0.87	1.70	0.19
Age	0.01	0.01	0.98	0.32
Lynch	0.37	0.33	1.25	0.26
FAP	2.65	0.76	12.15	4.9e-04

FAP, familial adenomatous polyposis; GEE, generalized estimating equation; LGR5, leucine-rich repeat–containing G-protein–coupled receptor 5.

healthy subjects and 2 subjects with FAP (10,11,14). Colocalization of LRIG1 and LGR5 staining was observed in healthy and FAP crypts (Figure 4b,d). Colocalization of BMI1 and LGR5 staining was observed in healthy crypts, but the same pattern was not seen in FAP crypts (Figure 4a,c). These results could suggest another aberrant feature of LGR5+ cells in normal-appearing crypts of subjects with FAP but need to be independently verified.

DISCUSSION

In this study, we demonstrated an increased number of LGR5+ stem cells in crypts of subjects with FAP compared with those of healthy subjects and subjects with Lynch syndrome. Furthermore, we observed crypts with ectopic LGR5+ cells more frequently in subjects with FAP than those in healthy subjects. However, this remains a qualitative observation without a more reliable and objective definition of ectopic. To our knowledge, this is the first study to examine individual LGR5+ cells in freshly isolated crypts from subjects with FAP. The increase in LGR5+ cell number was not observed in crypts of subjects with other forms of inherited risk of CRC, including Lynch syndrome and MAP. A potential consequence of this increased abundance of LGR5+ stem cells in crypts from subjects with FAP may be a higher number of proliferating transit amplifying cells with potential to develop mutations. The heightened mutation risk would in turn lead to an increased likelihood of developing premalignant conditions such as aberrant crypt foci and adenomatous polyps. Previous studies have identified an apically shifted proliferative zone in crypts of subjects with FAP and have suggested a WNT:APC inverse gradient that leads to ectopic and increased symmetrical stem cell division and overpopulation of stem cells when altered in FAP (27,36,37). Our results support the predictions of the inverse gradient model in the setting of *APC* haploinsufficiency but need to be independently validated.

This work also suggests a potential complementary diagnostic role for LGR5 quantification in the crypts of patients with suspected FAP. Despite advances in molecular genetic pathology, a recent search of the ClinVar database indicates that the pathogenicity of 3,102 of 4,910 (63%) documented single nucleotide variants in the *APC* gene is uncertain. Many of the variants of uncertain significance are rare or occur in noncoding regions with no obvious pathogenic effect. When genetic testing identifies a variant of uncertain significance in a patient suspected of having FAP, quantification of LGR5+ cells through immunostaining may serve a complementary role in assessing the phenotype and concomitant cancer risk. Although a higher throughput modality for quantifying LGR5+ cells will need to be developed before testing would be clinically useful, our findings may represent an opportunity to improve risk assessment in patients suspected of FAP.

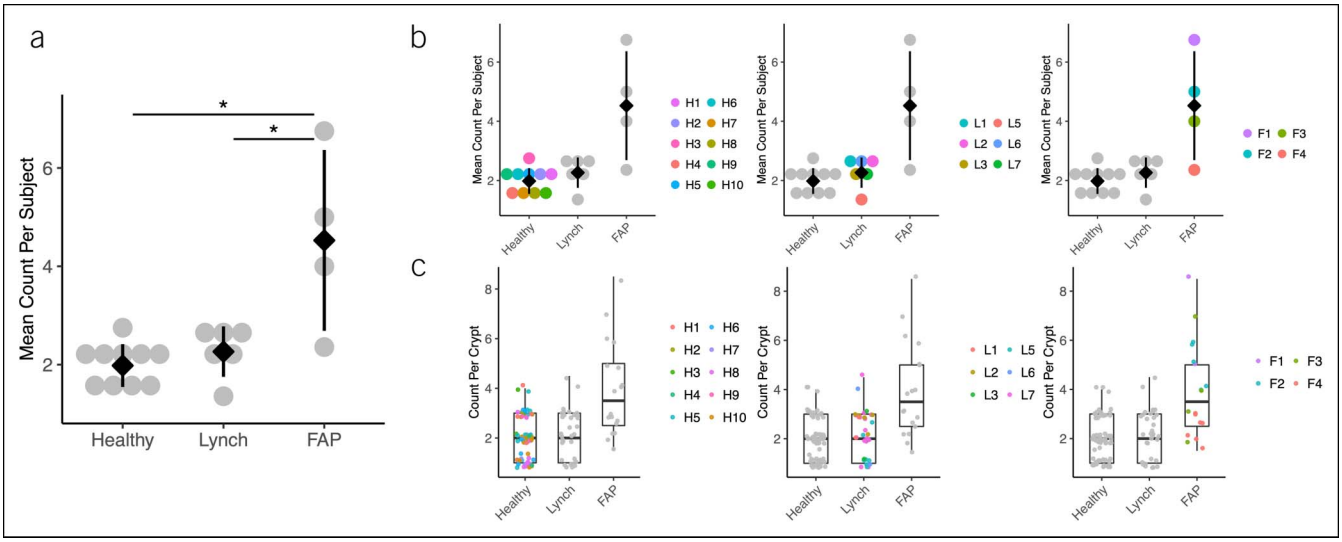

Figure 3. LGR5+ cell numbers in crypts of healthy subjects and subjects with Lynch syndrome and FAP. Summary of statistical comparison of LGR5+ cell abundance across groups. (**a**) Dot plot overlaid with group mean (black diamond) and standard deviation (black vertical bars) for subjects with FAP and Lynch syndrome and healthy subjects. Each gray dot represents the subject-specific mean across crypts for that subject. **P* value from generalized estimating equations estimate of coefficient (i.e., effect) of clinical diagnosis in model of cell count is less than 0.01. (**b**) Same dot plot as (**a**) with subjects labeled by color. (**c**) Crypt level counts for each subject represented by histograms within groups with points indicating the LGR5+ cell count in every crypt, with subjects labeled by color. In histograms, the thin box represents the within-group interquartile range, the thick horizontal line represents the median, and the thin vertical bars extend to points 1.5 times the interquartile range. Small increments of random noise have been added to points to facilitate visualization. Color labels in (**c**) are different from labels in (**b**). FAP, familial adenomatous polyposis; LGR5, leucine-rich repeat–containing G-protein–coupled receptor 5.

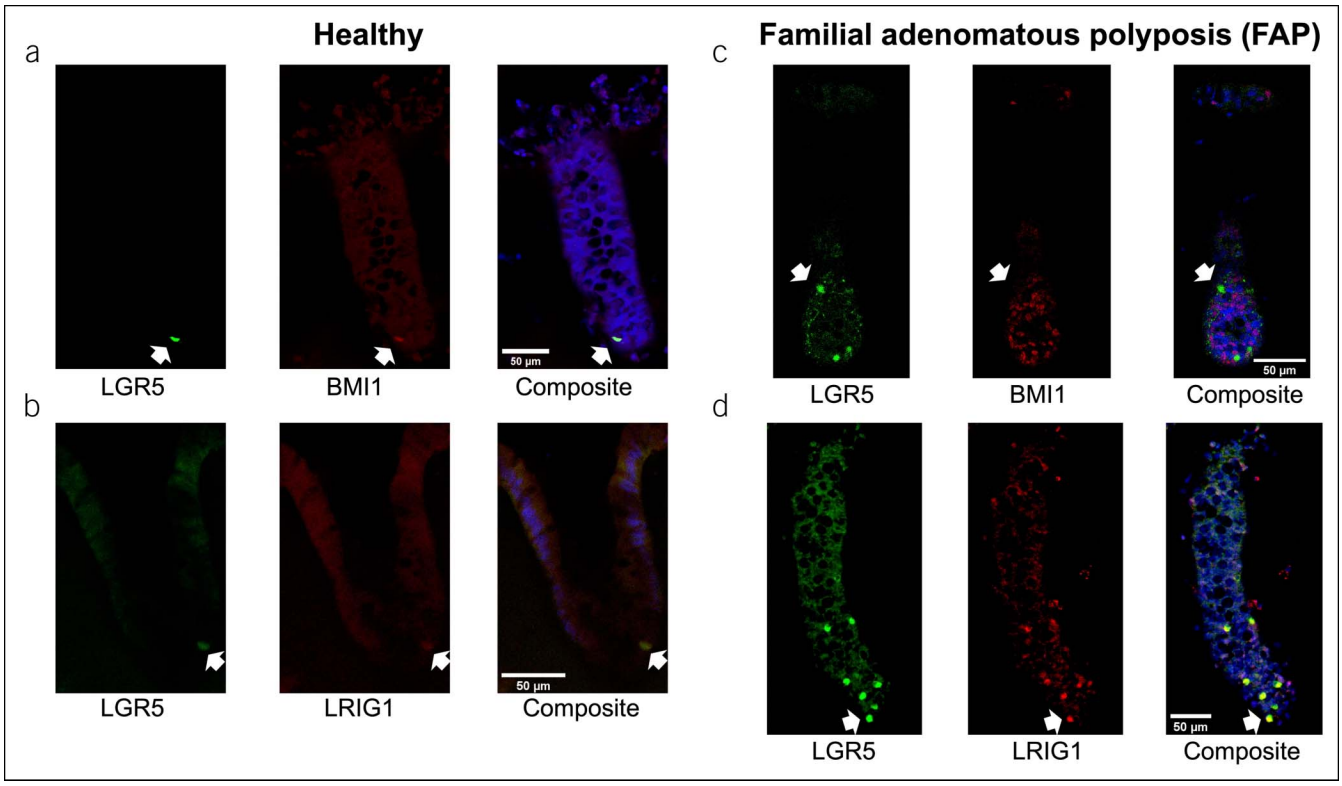

Figure 4. Staining of LGR5 and other stem cell markers in crypts of healthy subjects and subjects with FAP. Stem cell marker expression in normal colon crypts of healthy subjects and subjects with FAP. Arrows indicate location of representative LGR5+ cells. Blue is nuclear DNA counterstained with DAPI. (**a** and **b**) Immunofluorescence of LGR5 and LRIG1 or BMI1 in crypts of healthy subjects. (**c** and **d**) Immunofluorescence of LGR5 and LRIG1 or BMI1 in crypts of subjects with FAP. Objective: 20×. Scale bar: 50 μM. DAPI, 4′,6-diamidino-2-phenylindole; FAP, familial adenomatous polyposis; LGR5, leucine-rich repeat–containing G-protein–coupled receptor 5.

This work also highlights what may be the earliest histologically detectable premalignant change in crypts of subjects with FAP. For 3 of 4 subjects with FAP, the number of LGR5+ cells was substantially higher than for healthy subjects, but we report 1 case of a young (19 years) subject with FAP whose crypts displayed an intermediate quantity of LGR5+ cells. Crypts from this subject had higher numbers of LGR5+ cells, on average, than most crypts from healthy subjects but not as many as from older subjects with FAP, including a family member with the same germline *APC* mutation. Whether the number of LGR5+ cells increases over time in subjects with FAP or there is a wide range in LGR5+ cell number across subjects remains to be determined.

We note that our healthy cohort is older than our FAP cohort. An age-related decrease in LGR5 expression would be consistent with age-related epigenetic silencing of *Lgr5* mRNA transcription observed in intestinal organoids derived from aged mice (38) and could explain lower LGR5+ cell numbers in our healthy cohort. Although we cannot rule out the possibility that age differences contributed to our finding, we believe an increase in LGR5+ cell number in FAP is due to *APC* haploinsufficiency as opposed to younger age for 3 reasons. First, the highest number of LGR5+ cells in our FAP cohort was observed in the oldest subject. Second, no statistically significant association between LGR5+ cell count and age was observed in our healthy cohort (age range 52–74 years). Finally, subjects with Lynch syndrome younger than 40 years displayed LGR5+ cell numbers similar to healthy subjects. Our conclusion that an overabundance of LGR5+ cells in FAP crypts is associated with APC deficiency is consistent with Wnt-driven restoration of proliferative activity observed in intestinal organoids derived from aged mice (39).

Small sample size is the greatest limitation to this study. Because of the uninformative staining for LGR5 by immunohistochemistry in paraffin-embedded tissue and a steep attenuation in immunofluorescence staining in fresh biopsies over time, the study was restricted to fresh tissue collected at point of care. Given the relative infrequency of FAP in the general population, tissue from only 4 subjects with FAP was available. Furthermore, because of the older age of healthy subjects undergoing screening colonoscopies, quantification of LGR5+ cells in young, healthy subjects was not possible. To mitigate the key weaknesses of this study, multiple validations of LGR5 staining patterns were sought. Inclusion of 3 subjects with Lynch syndrome who were younger than 40 years permitted a limited assessment of crypts from younger subjects without FAP. This study should be expanded to determine whether improved stem cell markers and stains could be more amenable to immunohistochemical approaches for higher diagnostic throughput.

Our principal discovery was that the crypts of subjects with FAP, but not other CRC predisposition syndromes, exhibited a greater number of LGR5+ stem cells than crypts of healthy subjects. We also found that FAP crypts frequently harbored ectopic LGR5+ cells. These findings support a model in which inactivation of one copy of *APC* leads to increased LGR5+ stem cells in crypts that could eventually have prognostic value for

patients with polyposis and helps explain the FAP phenotype. Dysregulated proliferating cells may be more likely to develop mutations leading to the accelerated adenoma development observed in FAP.

CONFLICTS OF INTEREST

Guarantor of the article: Graham Casey, PhD.

Specific author contributions: Lucas T. Jennelle, PhD, and Christopher H. Dampier, MD, contributed equally to this study. L.T.J.: designed the study, collected and prepared specimens, performed microscopy, processed images, and wrote the manuscript. C.H.D.: contributed to study design, selected and analyzed images, performed statistical tests, and wrote the manuscript. S.T.: made original observations of stem cell enrichment in FAP crypts, contributed to study design, and edited the manuscript. S.P.: recruited subjects, collected biopsies, and edited the manuscript. G.C.: designed the study, interpreted the data, and wrote the manuscript.

Financial support: Funding for this work was provided by the following NIH Grants: R01 NIH/NCI CA143237 (G.C.) and T32 5T32CA163177-07 (Craig Slingluff, MD).

Potential competing interests: None to report.

ACKNOWLEDGEMENTS

We thank Stacey Criswell of the Advanced Microscopy Facility for expert assistance establishing confocal microscopy protocols. We also wish to acknowledge expert contribution of Patcharin Pramoonjago to immunohistochemistry, processing and staining FFPE samples, and validating antibody staining protocols. Tissue embedding for FFPE was conducted by expert histotechnologist Angela Miller. We are grateful to Sarah Plummer for offering to score crypts as an impartial observer. Finally, we wish to express immense gratitude toward all subjects who consented to participate in this study.

Study Highlights

WHAT IS KNOWN

- ✓ Colon crypts from subjects with familial adenomatous polyposis (FAP) harbor an expanded proliferative zone.
- ✓ LGR5+ stem cells of the colon are confined to the crypt base in healthy subjects.

WHAT IS NEW HERE

- ✓ Crypts from subjects with FAP, although morphologically normal in appearance, contain more LGR5+ cells than crypts from subjects without FAP.
- ✓ Crypts from subjects with FAP have ectopic LGR5+ cells more frequently than crypts from subjects without FAP.

TRANSLATIONAL IMPACT

- ✓ Preliminary evidence suggests quantification of LGR5+ cells in the crypts of subjects with suspected FAP has the potential to be a useful complement to genetic testing in evaluating cancer risk.

REFERENCES

1. McDonald SAC, Preston SL, Lovell MJ, et al. Mechanisms of disease: From stem cells to colorectal cancer. Nat Clin Pract Gastroenterol Hepatol 2006;3(5):267–74.
2. Vaiopoulos AG, Kostakis ID, Koutsilieris M, et al. Colorectal cancer stem cells. Stem Cells 2012;30(3):363–71.
3. Leedham SJ, Schier S, Thliveris AT, et al. From gene mutations to tumours - stem cells in gastrointestinal carcinogenesis. Cell Prolif 2005;38(6): 387–405.
4. Leedham SJ, Wright NA. Expansion of a mutated clone: From stem cell to tumour. J Clin Pathol 2008;61(2):164–71.
5. King JB, von Furstenberg RJ, Smith BJ, et al. CD24 can be used to isolate $Lgr5^{+}$ putative colonic epithelial stem cells in mice. Am J Physiol Gastrointestinal Liver Physiol 2012;303(4):G443–52.
6. Gracz AD, Fuller MK, Wang F, et al. Brief report: CD24 and CD44 mark human intestinal epithelial cell populations with characteristics of active and facultative stem cells: FACS enrichment of human intestinal stem cells. Stem Cells 2013;31(9):2024–30.
7. Dalerba P, Kalisky T, Sahoo D, et al. Single-cell dissection of transcriptional heterogeneity in human colon tumors. Nat Biotechnol 2011;29(12):1120–7.
8. Ke J, Wu X, Wu X, et al. A subpopulation of CD24+ cells in colon cancer cell lines possess stem cell characteristics. neo 2012;59(03):282–8.
9. Levin TG, Powell AE, Davies PS, et al. Characterization of the intestinal cancer stem cell marker CD166 in the human and mouse gastrointestinal tract. Gastroenterology 2010;139(6):2072–82.e5.
10. Powell AE, Wang Y, Li Y, et al. The pan-ErbB negative regulator Lrig1 is an intestinal stem cell marker that functions as a tumor suppressor. Cell 2012;149(1):146–58.
11. Wong VWY, Stange DE, Page ME, et al. Lrig1 controls intestinal stem-cell homeostasis by negative regulation of ErbB signalling. Nat Cell Biol 2012; 14(4):401–8.
12. van der Flier LG, Haegebarth A, Stange DE, et al. OLFM4 is a robust marker for stem cells in human intestine and marks a subset of colorectal cancer cells. Gastroenterology 2009;137(1):15–7.
13. Jung P, Sommer C, Barriga FM, et al. Isolation of human colon stem cells using surface expression of PTK7. Stem Cell Rep 2015;5(6):979–87.
14. Sangiorgi E, Capecchi MR. Bmi1 is expressed in vivo in intestinal stem cells. Nat Genet 2008;40(7):915–20.
15. Huang EH, Hynes MJ, Zhang T, et al. Aldehyde dehydrogenase 1 is a marker for normal and malignant human colonic stem cells (SC) and tracks SC overpopulation during colon tumorigenesis. Cancer Res 2009; 69(8):3382–9.
16. Baker AM, Graham TA, Elia G, et al. Characterization of LGR5 stem cells in colorectal adenomas and carcinomas. Sci Rep 2015;5(1):8654.
17. Becker L, Huang Q, Mashimo H. Immunostaining of Lgr5, an intestinal stem cell marker, in normal and premalignant human gastrointestinal tissue. Sci World J 2008;8:1168–76.
18. Dame MK, Attili D, McClintock SD, et al. Identification, isolation and characterization of human LGR5-positive colon adenoma cells. Development 2018;145(6):dev153049.
19. Reynolds A, Wharton N, Parris A, et al. Canonical Wnt signals combined with suppressed TGFβ/BMP pathways promote renewal of the native human colonic epithelium. Gut 2014;63(4):610–21.
20. Dame MK, Jiang Y, Appelman HD, et al. Human colonic crypts in culture: Segregation of immunochemical markers in normal versus adenoma-derived. Lab Invest 2014;94(2):222–34.
21. Barker N, van Es JH, Kuipers J, et al. Identification of stem cells in small intestine and colon by marker gene Lgr5. Nature 2007;449(7165): 1003–7.
22. Sato T, Vries RG, Snippert HJ, et al. Single Lgr5 stem cells build crypt-villus structures in vitro without a mesenchymal niche. Nature 2009; 459(7244):262–5.
23. Mahe MM, Aihara E, Schumacher MA, et al. Establishment of gastrointestinal epithelial organoids. Curr Protoc Mouse Biol 2013;3(4): 217–40.
24. Half E, Bercovich D, Rozen P. Familial adenomatous polyposis. Orphanet J Rare Dis 2009;4(1):22.
25. Ma H, Brosens LAA, Offerhaus GJA, et al. Pathology and genetics of hereditary colorectal cancer. Pathology 2018;50(1):49–59.
26. Mills SJ, Shepherd NA, Hall PA, et al. Proliferative compartment deregulation in the non-neoplastic colonic epithelium of familial adenomatous polyposis. Gut 1995;36(3):391–4.

27. Boman BM, Fields JZ. An APC:WNT counter-current-like mechanism regulates cell division along the human colonic crypt axis: A mechanism that explains how APC mutations induce proliferative abnormalities that drive colon cancer development. Front Oncol 2013;3:244.
28. Boman BM, Walters R, Fields JZ, et al. Colonic crypt changes during adenoma development in familial adenomatous polyposis: Immunohistochemical evidence for expansion of the crypt base cell population. Am J Pathol 2004;165(5):1489–98.
29. Yan J. geepack: Yet another package for generalized estimating equations. R-News 2002:12–4.
30. Yan J, Fine J. Estimating equations for association structures. Stat Med 2004;23(6):859–74; discussion 875–7, 879–80.
31. Halekoh U, Hojsgaard S, Yan J. The R package geepack for generalized estimating equations. J Stat Softw 2006;15(2):1–11.
32. R Core Team. R: A Language and Environment for Statistical Computing. R Foundation for Statistical Computing: Vienna, Austria, 2019.
33. Liang KY, Zeger SL. Longitudinal data-analysis using generalized linear-models. Biometrika 1986;73(1):13–22.
34. Wickham H. ggplot2: Elegant Graphics for Data Analysis. Springer-Verlag: New York, 2016.
35. Rothenberg ME, Nusse Y, Kalisky T, et al. Identification of a CKit(+) colonic crypt base secretory cell that supports Lgr5(+) stem cells in mice. Gastroenterology 2012;142(5):1195–205.e6.
36. Boman BM, Fields JZ, Cavanaugh KL, et al. How dysregulated colonic crypt dynamics cause stem cell overpopulation and initiate colon cancer. Cancer Res 2008;68(9):3304–13.
37. Baker AM, Cereser B, Melton S, et al. Quantification of crypt and stem cell evolution in the normal and neoplastic human colon. Cell Rep 2014;8(4):940–7.
38. Uchida R, Saito Y, Nogami K, et al. Epigenetic silencing of Lgr5 induces senescence of intestinal epithelial organoids during the process of aging. NPJ Aging Mech Dis 2019;5(12):1.
39. Nalapareddy K. Canonical Wnt signaling ameliorates aging of intestinal stem cells. Cell Rep 2017;18(11):2608–21.